Modeling and Control of Marine Current Turbines and Energy Storage Systems ⋆

Aoife Nic Einrí * **Gudrún Margrét Jónsdóttir** *
Federico Milano *

* *School of Electrical & Electronic Engineering*
University College Dublin, Ireland
e-mails: aoife.nic-einri@ucdconnect.ie;
gudrun.jonsdottir@ucdconnect.ie; federico.milano@ucd.ie.

Abstract: Swells in the marine current can cause unanticipated fluctuations in the power generated by Marine Current Turbines (MCTs). While the marine current in a single point under swell effect can be captured through a well-defined model, realistic aggregated models that capture the spatial distribution of the turbines that compose a MCT farm have not been proposed yet. This paper aims at filling this gap. The proposed model also helps design Energy Storage Systems (ESSs) included in MCT farms to level the power fluctuations caused by swells. Results highlight that there is the need for more detailed models of the correlation of marine currents in a farm of MCTs.

Keywords: Marine current turbine (MCT), swell effect, energy storage system (ESS)

1. INTRODUCTION

1.1 Motivations

Ocean-based renewable energy sources exist in various forms, i.e. tidal, wave and thermal energy. Among these, tidal energy is considered to be the most promising [WEC (2016)]. Tidal generation is dependent on marine current. The marine current can be subjected to short-term fluctuations due to swells in the ocean. These fluctuations can effect the power quality and stability of power systems. The swells in the current in a single point have been modeled in the literature. However, the aggregated current of a MCT farm has not been modeled and is therefore the subject of this paper.

1.2 Literature Review

One of the main advantages of marine current energy compared to other prominent renewable energy sources (wind, solar, etc) is its high predictability. This is because marine currents are mostly driven by the tidal phenomenon, which depends on astronomical forces making it predictable within 98% accuracy [Benelghali et al. (2011)]. However, the marine current speed is subject to short-term disturbances caused by the swell phenomenon. The fluctuations in the power originated by the swell can be viewed as *forced oscillations* that need to be effectively damped to ensure a stable and reliable operation of the system [Ghorbaniparvar (2017)].

The Stokes model coupled with the JONSWAP spectrum [Zhou et al. (2013a); Anwar et al. (2016); Zhou et al. (2013b)] is typically utilized to model the swell effect in one point. This model captures the effect of swells for a single turbine, not a whole park of MCTs. The aggregation of the marine current for a park of MCTs remains an open research question.

Coupled with the issue of properly modeling the swell effect, there is the need to design an effective control to reduce active power fluctuations. An efficient solution is to install a ESS at the point of connection of the MCT farm with the grid. With this regard, several energy storage technologies have been discussed in the literature. In [Zhou et al. (2013b); Pham et al. (2017)], electrochemical capacitors are proposed and in [Anwar et al. (2016)] lithium-ion batteries. These publications have identified the size of the ESS to have to be approximately half of the size of the MCT farm if no additional control is used. However, references [Anwar et al. (2016); Zhou et al. (2013b); Pham et al. (2017)] can be prone to overestimate the capacity of the storage device because a detailed model of the aggregated MCT farm current is not considered.

1.3 Contributions

The goal of this paper is to understand the limitations of single-point models of marine currents for MCT power plants. The specific contributions of this paper are threefold:

- Propose an approach to aggregate the marine current speed of a MCT farm.
- Study the effect of the swell phenomenon on a modified 9-bus 3-machine test system for the worst and best case scenario of swells.
- Discuss the design of ESSs for levelling the swell-induced power fluctuations.

⋆ This material is based upon works supported by the Science Foundation Ireland, under Investigator Programme, Grant No. SFI/15/IA/3074.

1.4 Paper Organisation

The remainder of the paper is organized as follows. Section 2 outlines the model of the marine system, including marine current, aggregated current and the generator model. In Section 3 the ESS used to smooth the power fluctuations induced by swells is presented. The case study is outlined in Section 4 and further discussion on the results are provided in Section 5. Finally, in Section 6 conclusions are drawn and future work is outlined.

2. MARINE SYSTEM MODELING

In this section, the components of the implemented marine system model are presented. First the marine current model for a single turbine with the swell-induced short term oscillations is presented in Section 2.1. An aggregated marine current model is proposed in Section 2.2 to better represent the effective marine current in a park of MCTs. The aggregated marine current is the input to the aggregated marine generator model outlined in Section 2.3.

2.1 Current speed models

Two kinds of periodical fluctuations can be identified in the marine current. On a daily time scale the current varies with a period of 6 or 12 hours due to the tidal astronomical phenomenon. These fluctuations are highly predictable. On a smaller time scale, that is in a matter of seconds, the marine current fluctuates due to wind waves and ocean swells. It is the swell induced fluctuations that are of interest in this paper.

Swells are long wavelength waves that originate in a remote region of the ocean and propagate out of their area of generation. The intensity of the swell waves varies as they move through the ocean. Low frequency components of the wave propagate faster than the high ones. Therefore, the swell effect at a fixed point has a narrow frequency spectrum characterized by a sharp peak.

The JONSWAP spectrum is a well-accepted analytical model for the swell wave spectrum [Hasselmann et al. (1973)]:

$$S(\omega) = \frac{\alpha g^2}{\omega^5} \exp\left(-\beta \left(\frac{\omega_p}{\omega}\right)^4 \right) \gamma^Y \ , \tag{1}$$

where ω is the wave angle frequency, α is the intensity of the spectra, g is the acceleration due to gravity, β is the shape factor and ω_p is the frequency at the peak of the spectrum. The parameter γ is the peak enhancement factor which controls the sharpness of the peak and

$$Y = \exp\left(-\left(\frac{\omega - \omega_p}{\sqrt{2}\omega_p \sigma}\right)^2 \right) \ , \tag{2}$$

where

$$\sigma = \begin{cases} 0.07 \text{ if } \omega \leq \omega_p \\ 0.09 \text{ if } \omega > \omega_p \ . \end{cases} \tag{3}$$

The JONSWAP spectrum used in this paper is shown in Fig. 1. It has a sharp peak and a narrow frequency range as is the case for swell waves. Based on the swell spectrum, the horizontal current velocity can be derived through the super positioning of m frequency components.

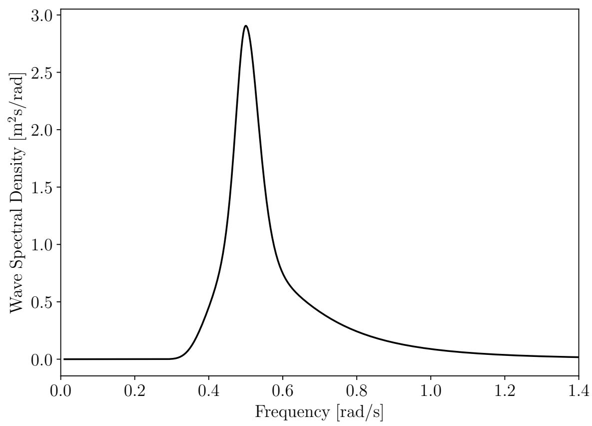

Fig. 1. The JONSWAP spectrum.

The first order Stokes model is used to model the marine current. The marine current is represented through the following combination of the tidal speed and the swell effect:

$$u_j(t) = u_{\text{tide}} + \sum_{i=1}^{m} \omega_i a_i \frac{\cosh(k_i(z+d))}{\sinh(k_i(z+d))} \cos(\omega_i t + \phi_i) \ . \tag{4}$$

Above, u_{tide} represents the predicted tidal speed (which is taken to be the zero-frequency component of any current model and constant in the case study in Section 4). With

$$a_i = \sqrt{2S(\omega_i)\Delta\omega_i} \ , \tag{5}$$

being the amplitude of the i-th frequency component defined from the JONSWAP spectrum (1); ω_i is the frequency of the i-th component, k_i is the wave number of the i-th component, z is the vertical distance from the sea surface to the hub height of the MCT, d is the depth from the ocean floor and ϕ_i is the initial phase angle of the i-th frequency component.

2.2 Aggregated Current Model

The model in (4) captures the marine current for a single MCT. Most often, a number of MCTs are installed close to each other to form a park of MCTs. An aggregated generator model is used to represent all the turbines in the park using a single generator (see Section 2.3). To account for the averaging effect of considering the MCT park as a whole an aggregated model for the current speed is proposed in this paper. This model is based on a similar model used for aggregating wind turbines [Rousi et al. (2014)].

The aggregated marine current for n individual currents is:

$$u_{\text{agg}}(t) = \sum_{k=1}^{n} u_{j_n}(t)/n \ , \tag{6}$$

where the n marine currents $u_{j_n}(t)$ are defined in (4). All n current models have identical parameters except for the phase angle. The phase angle of each frequency component of each current is a uniformly distributed random number, that is $\phi_{i_n} \sim \mathcal{U}(0, 2\pi)$.

2.3 Tidal turbine farm model

Numerous devices to harvest energy from tidal streams are available in the literature. The main research focus is on horizontal-axis turbines as 75 % of all R&D investments in ocean energy is dedicated to their development [WEC (2016)]. A contributing factor for their dominance is their similarity to wind turbines. This allows much of the readily available technology for wind generation to be reused for MCTs. The MCT model used in this paper is a single aggregated model that represents a whole farm of n_{gen} MCTs.

Turbine model For MCTs the power extracting principle is similar to wind turbines. The power $p_m(t)$ extracted from the marine current is a function of the marine current $v_m(t)$, that is:

$$p_m(t) = \frac{1}{2} n_{\text{gen}} \rho \eta_m(\lambda_t(t), \beta_p(t)) A_r v_m^3(t) \ . \qquad (7)$$

where $\eta_m(\lambda_t(t), \beta_p(t))$ is the performance coefficient that measures the efficiency of the marine turbine. Where $\beta_p(t)$ is the blade pitch angle and $\lambda_t(t) = v_{bt}(t)/v_m(t)$ is the tip speed ratio that is the ratio between the blade tip speed $v_{bt}(t)$ and the actual marine current speed. $A_r = \pi r^2$ is the swept area of the rotor, with r as the rotor radius. n_{gen} is the total number of generators in the aggregated model and ρ is the sea water density.

Generator model The MCT generator is represented using the double-fed induction generator (DFIG), see Fig. 2. It consists of an induction machine, an AC/AC power converter connecting the rotor and the stator and includes the controls presented in Section 2.3.3.

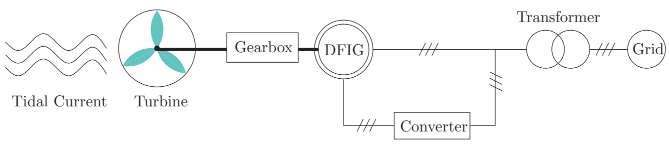

Fig. 2. DFIG scheme [Zhang et al. (2014)].

The generator dynamic model used written in the synchronously rotating dq frame is given by the following equations. The voltage equations are:

$$\begin{aligned} V_{sd} &= R_s I_{sd} + \frac{d\phi_{sd}}{dt} - \omega_s \phi_{sq} \\ V_{sq} &= R_s I_{sq} + \frac{d\phi_{sq}}{dt} + \omega_s \phi_{sd} \\ V_{rd} &= R_r I_{rd} + \frac{d\phi_{rd}}{dt} - \omega_r \phi_{rq} \\ V_{rq} &= R_r I_{rq} + \frac{d\phi_{rq}}{dt} + \omega_r \phi_{rd} \ ; \end{aligned} \qquad (8)$$

the generator flux is defined as:

$$\begin{aligned} \phi_{sd} &= -L_s I_{sd} - L_m I_{rd} \\ \phi_{sq} &= -L_s I_{sq} - L_m I_{rq} \\ \phi_{rd} &= -L_r I_{rd} - L_m I_{sd} \\ \phi_{rq} &= -L_r I_{rq} - L_m I_{sq} \ ; \end{aligned} \qquad (9)$$

and the mechanical equations of the generator are:

$$\begin{aligned} T_{em} &= \frac{3}{2} p L_m (I_{sq} I_{rd} - I_{sd} I_{rq}) \\ J\frac{d\omega_m}{dt} &= T_{em} - T_m - f\omega_m \ . \end{aligned} \qquad (10)$$

In (8)-(10), s and r indicate stator and rotor quantity, respectively, d and q signify a d-axis and q-axis quantity, respectively, V is a voltage (V), R is a resistance (Ω), I is a current (A), ϕ is a flux (Wb), L is a mutual inductance (H), f is the combined rotor and load friction coefficient, T_{em}, T_m are the electromagnetic and shaft mechanical torque, respectively (Nm), J is the combined rotor and load inertia coefficient (kgm^2), ω, ω_s, $\omega_r = \omega_s - \omega$ are the rotor electrical speed, synchronous electrical speed and rotor current frequency, respectively (rad/s) and $\omega_m = \frac{\omega}{p}$ is the rotor mechanical angular velocity (rad/s), p is the number of poles.

Controllers

- **Pitch angle control:** The pitch angle of the MCT can vary from $0 - 180°$ because of its bi-directional operation caused by the flood and ebb. The pitch angle control applied prevents the turbine from rotating at a speed that exceeds a given limit ω_t^{ref}. This control diagram is shown in Fig. 3. It discretizes the variations of the pitch angle in terms of predefined $\Delta\omega$ steps. The control is activated when the rotor speed is greater than the rotor speed reference value ω_t^{ref}. An anti-windup limiter locks the pith angle to $\beta_p = \beta_{p,0}$ for $\omega_t \leq \omega_t^{\text{ref}}$.

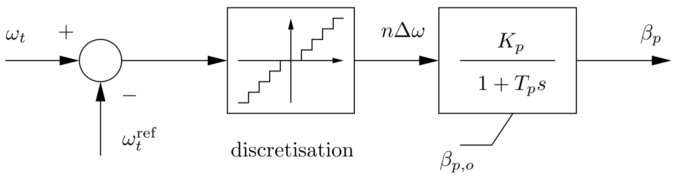

Fig. 3. Scheme of the pitch angle control.

- **Maximum Power Point Tracking (MPPT):** The MPPT provides speed control that aims to maximize the power production of the MCT. The power reference, p_m^{ref} of the MPPT is dependent on the rotor speed. For $\omega_t > \omega_t^{\max}$ ($\omega_t^{\max}$ is the generators maximum rotor speed) p_m^{ref} is kept constant to avoid over-speeding the generator and the turbine shaft. For $\omega_t < \omega_t^{\min}$ p_m^{ref} is set to zero. In the range $\omega_t^{\min} < \omega_t < \omega_t^{\max}$ the optimal p_m^{ref} can be approximated by a cubic polynomial, that is:

$$p_m^{\text{ref}}(t) = \begin{cases} 0 & \text{if } \omega_t(t) < \omega_t^{\min} \\ c_m \omega_t^3(t) & \text{if } \omega_t^{\min} \leq \omega_t(t) \leq \omega_t^{\max} \\ p_m^{\max} & \text{if } \omega_t(t) > \omega_t^{\max} \end{cases} \qquad (11)$$

where $c_w = p_m^*(\omega_t^{\min})/(\omega_t^{\min})^3$ and $p_m^*(\omega_t^{\min})$ is the maximum power at $\omega_t^{\min}$.

3. ENERGY STORAGE SYSTEM

The marine current source is typically considered favorable compared to other renewable sources such as wind and solar because of its predictability. However, the source also fluctuates both in a short-time frame (due to swells) and in a long-time frame (due to the tidal phenomenon). These fluctuations make it difficult for the system operator to stabilize the network and balance the supply and demand. Therefore, installing Energy Storage Systems (ESSs) alongside the marine generation is considered essential to smooth the output power of the MCTs [Zhou et al. (2013a)].

Two types of ESSs are typically discussed when it comes to marine generation. A long-term (several hours) and a short-term (several minutes) storage. The latter one is considered in this paper. In the literature, supercapacitors [Zhou et al. (2013a); Pham et al. (2017)], batteries [Anwar et al. (2016)] and flywheels [Zhou et al. (2013a)] have been suggested as options for short-term storage.

In this paper, a Flywheel Energy Storage System (FESS) is used as its features make it one of the best candidates for smoothing short-term fluctuations of MCT systems. To represent the FESS in the case study in Section 4 the simplified ESS model presented in Fig. 4 is used [Pal et al. (2000); Ortega and Milano (2016)]. The ESS is represented through decoupled active and reactive power controllers. The input signal ω is the local bus frequency that is regulated through the active power. The voltage at the point of connection v_{ac} is regulated through the ESS reactive power. The physical behavior of the storage system is synthesized by two lag blocks with the time constants $T_{P,\mathrm{ESS}}$ and $T_{Q,\mathrm{ESS}}$. In the case study $T_{P,\mathrm{ESS}} = 0.1$ s and $T_{Q,\mathrm{ESS}} = 0.01$ s to represent the FESS.

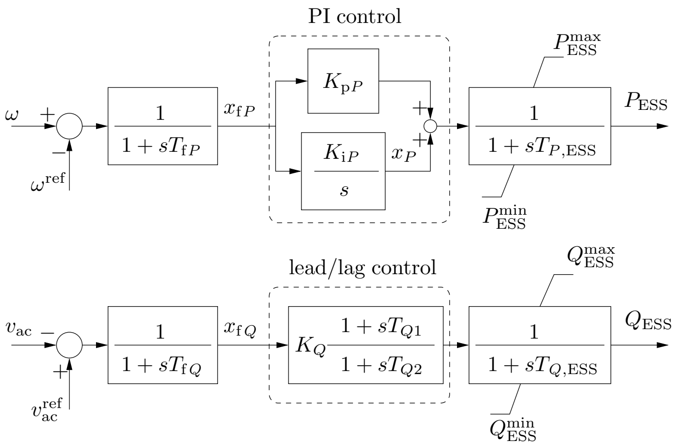

Fig. 4. The simplified ESS used in the case study.

4. CASE STUDY

The test power system used in this case study is the Western System Coordinating Council (WSCC) 3-machine, 9-bus system shown in Fig. 5 [Sauer and Pai (1997)]. The test system has three synchronous generators with Automatic Voltage Regulation (AVR), Power System Stabilizers (PSSs) and turbine governors. The test system is modified and a MCT power plant is connected at bus 7. Approximately 10% of the total generation of the system is relocated from the synchronous generator at Bus 2 to the MCT power plant.

All simulations in this Section were carried out using Dome, a Python-based software tool for power system analysis [Milano (2013)].

The total active power produced by the marine generator is 32.8 MW. Each individual MCT is set to generate about 1 MW. Therefore, the park consists of a total of 30 MCTs.

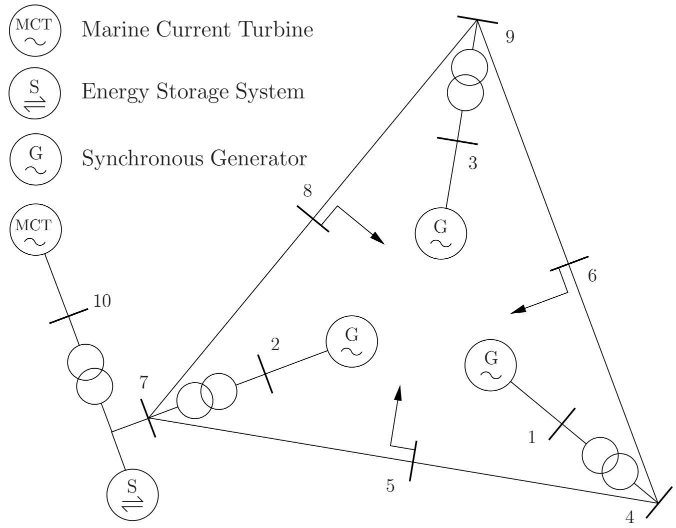

Fig. 5. The test power system used in the case study.

To assess the effect of the swells in the marine current on the system, both the marine current model in (4) and the aggregated model in (6) are used. In Fig. 6, the marine current for the following five different cases is shown:

- **Case 1:** Marine current without swell effect. This is the value for u_{tide} in the remaining cases.
- **Case 2:** The marine current generated using the model presented in (4).
- **Case 3-5:** The aggregated marine current in (6) for 5, 15 and 30 currents respectively.

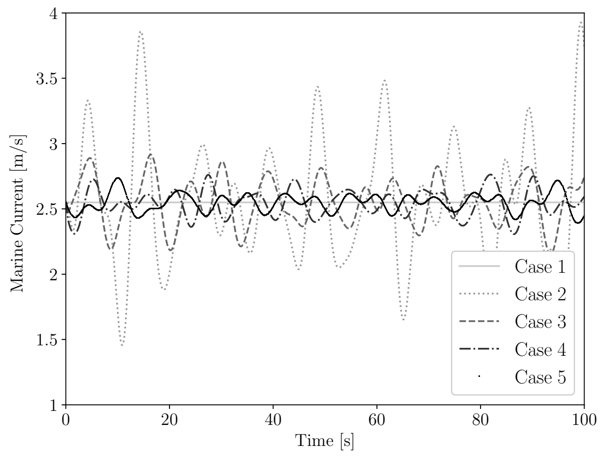

Fig. 6. The marine current for Case 1-5.

Case 2 and Case 5 represent the two extreme cases when the marine current is affected by swells. That is, in Case 2, it is assumed that the marine current is the same for all turbines in the park at the same time. Whereas, in Case 5, each turbine has an individual marine current with random phase angles ϕ_i in (4).

Figure 7 shows the generated power of the MCT park for Case 2 and Case 5. The averaging in the aggregated model significantly reduces the fluctuations in the generated power due to the swell effect. However, the fluctuations are not fully eliminated.

The periodical behavior of the power generated by the MCT introduces oscillations in the grid. These oscillations are categorized as forced oscillations as they are the systems response to an external periodical perturbation [Ghorbaniparvar (2017)]. In this case, the periodic perturbation is due to swells in the marine current. These oscillations can result in reduced power quality, equipment malfunction, improper operation and stability issues. Therefore, it is essential that these oscillations are smoothed.

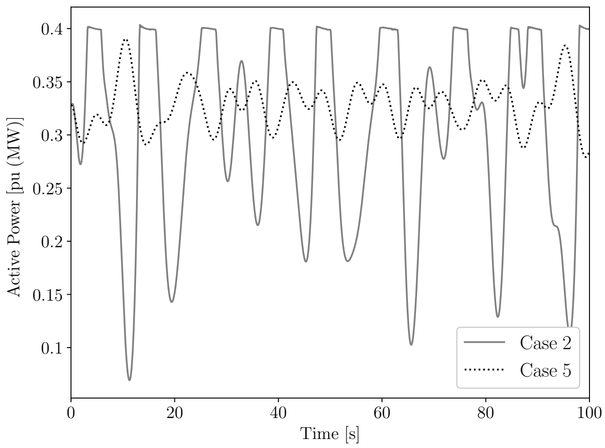

Fig. 7. The generated active power of the MCT power plant fed with the marine current for Case 2 and 5.

The effect of the swell-induced forced oscillations for both Case 2 and 5 on the COI frequency is shown in Fig. 8 and on the voltage at Bus 1 in Fig. 9. The significant difference in the size of the variations between the two extreme scenarios is evident. To better compare the two, the standard deviation of the COI frequency and the voltage at Bus 1 for both cases is shown in Table 1.

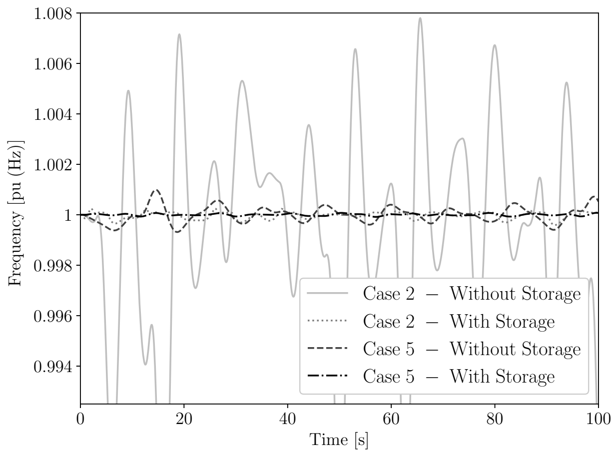

Fig. 8. The COI frequency for Case 2 and 5, with and without storage.

A FESS, as presented in Section 3 is installed at Bus 7 to smooth the oscillations. The required size of the storage varies significantly between the two extreme scenarios, namely Case 2 and 5. For the non-aggregated current

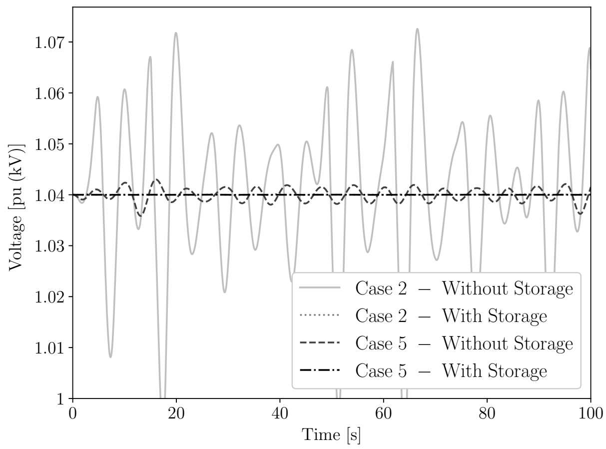

Fig. 9. The voltage at Bus 1 for Case 2 and 5, with and without storage.

Table 1. The standard deviation of frequency of the COI (σ_{COI}) and the voltage at Bus 1 (σ_{V_1}) for Cases 2 and 5 with and without storage.

Case	Storage	Standard deviation	
		σ_{COI} [pu (Hz)]	σ_{V_1} [pu (kV)]
2	No	$4.588 \cdot 10^{-3}$	$1.695 \cdot 10^{-2}$
2	Yes	$1.339 \cdot 10^{-4}$	$3.851 \cdot 10^{-5}$
5	No	$3.556 \cdot 10^{-4}$	$1.440 \cdot 10^{-3}$
5	Yes	$3.615 \cdot 10^{-5}$	$9.260 \cdot 10^{-6}$

model, Case 2, the active power fluctuations are up to 0.4 MW. On the other hand, for the aggregated model of Case 5, the fluctuations are 0.1 MW in magnitude, i.e. one fourth the value of Case 2 (see Fig. 7). In Case 2, the fluctuations are contained by the limits of the MCT power plant.

Figures 8 and 9 show that the oscillations in the frequency and voltage are significantly damped by the addition of the ESS for both Case 2 and 5. This is further demonstrated by comparing the standard deviations shown in Table 1.

5. DISCUSSION

In the literature, three studies have been conducted for utilizing ESS systems for power smoothing of MCT fluctuations caused by swells [Anwar et al. (2016); Zhou et al. (2013b); Pham et al. (2017)]. In [Zhou et al. (2013b)] and [Pham et al. (2017)], 1.5 MW MCT systems are studied and supercapacitor ESSs are used. The size of the ESS system is not specified in [Pham et al. (2017)] but the power fluctuations are shown to exceed the size of the MCT plant which indicates that the size of the ESS should be at least 1.5 MW. In [Zhou et al. (2013b)], the size of the ESS is set to 700 MW. The size of the ESS is relatively large but is assumed to be reasonable because the ESS cost would only be a fraction of the total cost of the marine system. Finally, in [Anwar et al. (2016)], a 15 MW marine generation is studied and a lithium-ion battery of the size 7 MW is used. The paper proposes using pitch angle control and inertial response to reduce the fluctuations so a smaller battery is needed. However, as all these studies consider the worst-case scenario (Case 2 in Section 4) the additional control for smoothing of these oscillations might be unnecessary. A more detailed model of the aggregated marine current can help design the appropriate size for the ESS.

In the case study discussed in Section 4, the two limit cases are examined (Case 2 and 5) and it is identified that the size of the ESS (intended for smoothing the fluctuations caused by the swell effect) for a 30 MW MCT farm should be somewhere in the range 100 – 400 kW. The aggregated model allows considering the boundary conditions of the ESS capacity requirements. The aggregated model presented in Section 2.2 is a starting point but detailed measurement data of marine currents flowing through a MCT farm are needed to define the capacity of the ESS. Relevant parameters to consider are the layout of the MCT farm, the wake effect and the correlation in the current between individual turbines.

6. CONCLUSIONS

The paper studies the effect of swells in marine current on power systems with MCTs. The swell effect on a single turbine is modeled using the first order Stokes model coupled with the JONSWAP spectrum. A simple model that takes into account the effect of aggregated marine currents on a MCT farm is proposed.

Swells cause fluctuations in the output power of MCT power plants. ESSs are effective to smooth these fluctuations. In this paper it is shown how the proposed aggregated model can be used to assist in better assessing the capacity of the ESS.

The proposed aggregation method suggests accurate data of marine currents in different locations are required to effectively decide the capacity of the installed ESS. Future work will seek such data and include the modeling of the marine currents considering the wake effect and the correlation in the current between individual turbines.

REFERENCES

Anwar, M.B., El Moursi, M.S., and Xiao, W. (2016). Dispatching and frequency control strategies for marine current turbines based on doubly fed induction generator. *IEEE Transactions on Sustainable Energy*, 7(1), 262–270.

Benelghali, S., Benbouzid, M.E.H., Charpentier, J.F., Ahmed-Ali, T., and Munteanu, I. (2011). Experimental validation of a marine current turbine simulator: Application to a PMSG-based system second-order sliding mode control. *IEEE Transactions Industrial Electronics*, 58(1), 118–126.

Ghorbaniparvar, M. (2017). Survey on forced oscillations in power system. *Journal of Modern Power Systems and Clean Energy*, 5(5), 671–682.

Hasselmann, K., Barnett, T., Bouws, E., Carlson, H., Cartwright, D., Enke, K., Ewing, J., Gienapp, H., Hasselmann, D., Kruseman, P., et al. (1973). Measurements of wind-wave growth and swell decay during the Joint North Sea Wave Project (JONSWAP). *Ergänzungsheft 8-12*.

Milano, F. (2013). A Python-based software tool for power system analysis. In *Power and Energy Society General Meeting (PES)*, 1–5. IEEE.

Ortega, Á. and Milano, F. (2016). Generalized model of VSC-based energy storage systems for transient stability analysis. *IEEE Transactions on Power Systems*, 31(5), 3369–3380.

Pal, B.C., Coonick, A.H., Jaimoukha, I.M., and El-Zobaidi, H. (2000). A linear matrix inequality approach to robust damping control design in power systems with superconducting magnetic energy storage device. *IEEE Transactions on Power Systems*, 15(1), 356–362.

Pham, H.T., Bourgeot, J.M., and Benbouzid, M. (2017). Power smoothing control and low-voltage ride-through enhancement of a 5-phase PMSG-based marine tidal turbine using a supercapacitor energy storage system. In *Industrial Electronics Society, IECON*, 8323–8328. IEEE.

Rousi, G., Hansen, A.D., and Cutululis, N.A. (2014). Wind farm aggregation method for dynamic active power studies. In *13th International Workshop on Large-Scale Integration of Wind Power into Power Systems as well as on Transmission Networks for Offshore Wind Power (WIW 2014)*.

Sauer, P.W. and Pai, M. (1997). Power system dynamics and stability. *Urbana*, 51, 61801.

WEC (2016). World Energy Council, World Energy Resources - Marine Energy 2016. URL `https://www.worldenergy.org`.

Zhang, J., Moreau, L., Machmoum, M., and Guillerm, P.E. (2014). State of the art in tidal current energy extracting technologies. In *International Conference on Green Energy*, 1–7. IEEE.

Zhou, Z., Benbouzid, M., Charpentier, J.F., Scuiller, F., and Tang, T. (2013a). A review of energy storage technologies for marine current energy systems. *Renewable and Sustainable Energy Reviews*, 18, 390–400.

Zhou, Z., Scuiller, F., Charpentier, J.F., Benbouzid, M.E.H., and Tang, T. (2013b). Power smoothing control in a grid-connected marine current turbine system for compensating swell effect. *IEEE Transactions on Sustainable Energy*, 4(3), 816–826.